

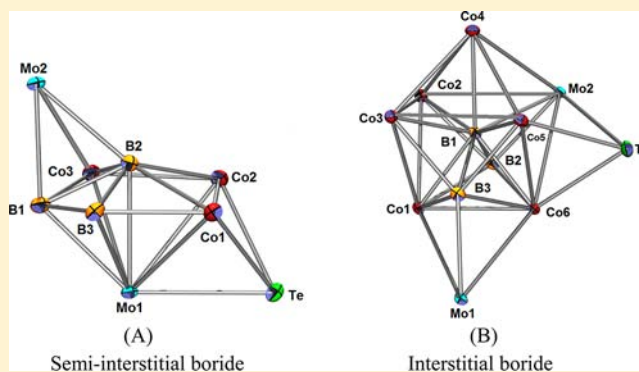
Novel Class of Heterometallic Cubane and Boride Clusters Containing Heavier Group 16 Elements

Arunabha Thakur, Soumik Sao, V. Ramkumar, and Sundargopal Ghosh*

Department of Chemistry, Indian Institute of Technology Madras, Chennai 600 036, India

S Supporting Information

ABSTRACT: Thermolysis of an in situ generated intermediate, produced from the reaction of $[\text{Cp}^*\text{MoCl}_4]$ ($\text{Cp}^* = \eta^5\text{-C}_5\text{Me}_5$) and $[\text{LiBH}_4\cdot\text{THF}]$, with excess Te powder yielded isomeric $[(\text{Cp}^*\text{Mo})_2\text{B}_4\text{TeH}_5\text{Cl}]$ (**2** and **3**), $[(\text{Cp}^*\text{Mo})_2\text{B}_4(\mu_3\text{-OEt})\text{TeH}_3\text{Cl}]$ (**4**), and $[(\text{Cp}^*\text{Mo})_4\text{B}_4\text{H}_4(\mu_4\text{-BH})_3]$ (**5**). Cluster **4** is a notable example of a dimolybdaoxatelluraborane cluster where both oxygen and tellurium are contiguously bound to molybdenum and boron. Cluster **5** represents an unprecedented metal-rich metallaborane cluster with a cubane core. The dimolybdaheteroborane **2** was found to be very reactive toward metal carbonyl compounds, and as a result, mild pyrolysis of **2** with $[\text{Fe}_2(\text{CO})_9]$ yielded distorted cubane cluster $[(\text{Cp}^*\text{Mo})_2(\text{BH})_4(\mu_3\text{-Te})\{\text{Fe}(\text{CO})_3\}]$ (**6**) and with $[\text{Co}_2(\text{CO})_8]$ produced the bicapped pentagonal bipyramid $[(\text{Cp}^*\text{MoCo})_2\text{B}_3\text{H}_2(\mu_3\text{-Te})(\mu\text{-CO})\{\text{Co}_3(\text{CO})_6\}]$ (**7**) and pentacapped trigonal prism $[(\text{Cp}^*\text{MoCo})_2\text{B}_3\text{H}_2(\mu_3\text{-Te})(\mu\text{-CO})_4\{\text{Co}_6(\text{CO})_8\}]$ (**8**). The geometry of **8** is an example of a heterometallic boride cluster in which five Co and one Mo atom define a trigonal prismatic framework. The resultant trigonal prism core is in turn capped by two boron, one Te, and one Co atom. In the pentacapped trigonal prism unit of **8**, one of the boron atoms is completely encapsulated and bonded to one molybdenum, one boron, and five cobalt atoms. All the new compounds have been characterized in solution by IR, ^1H , ^{11}B , and ^{13}C NMR spectroscopy, and the structural types were unambiguously established by crystallographic analysis of **2** and **4–8**



INTRODUCTION

Boron, being the only nonmetal element in group 13, forms a number of different clusters with both main group and transition metal elements. Over the past few decades, extensive efforts have been made to synthesize mixed-metal chalcogenide clusters of high nuclearity, and exploitation of new cluster components continues to be an imperative stage for accomplishing large-core structures.¹ Transition metal–chalcogen chemistry that deals with compounds containing a cubane-type core and in which the metal and chalcogen atoms occupy adjacent vertices is a unique area of research. These compounds are of interest not only because of their contribution to the growth of modern organometallic chemistry but also for their potential use as models for various industrial and biological catalytic processes.^{2–4}

A continuous research interest in our laboratory has been the synthesis and structural characterization of cubane or boride clusters containing transition metal and chalcogen atoms. As shown in Chart 1, a number of such species have recently been synthesized from the thermolysis of $[(\text{Cp}^*\text{Mo})_2\text{B}_4\text{E}_2]$ ($\text{E} = \text{S}, \text{Se}$) in the presence of $[\text{Fe}_2(\text{CO})_9]$, which generates cubane-type clusters $[(\text{Cp}^*\text{Mo})_2(\mu_3\text{-E})_2\text{B}_2\text{H}(\mu\text{-H})\{\text{Fe}(\text{CO})_2\}_2\text{Fe}(\text{CO})_3]$, **I** and **II** (**I**: $\text{E} = \text{S}$; **II**: $\text{E} = \text{Se}$).⁵ In a similar fashion, reaction of $[(\text{Cp}^*\text{CO})_2\text{-}arachno\text{-Ru}_2\text{B}_2\text{H}_6]$ with excess $[\text{Fe}_2(\text{CO})_9]$ resulted in the formation of $[(\text{Cp}^*\text{Ru})_2(\mu_3\text{-$

$\text{CO})_2\text{B}_2\text{H}(\mu\text{-H})\{\text{Fe}(\text{CO})_2\}_2\text{Fe}(\text{CO})_3]$, **III**, similar to the geometry of **I** and **II**.⁵ Although homometallic and heterometallic cubane clusters containing chalcogen elements are well documented in the literature,^{6–8} up until now only a few cubane clusters containing boron as a main group element are known^{9,10} (Chart 1). In addition, structurally characterized metallaheteroboranes having a cubane core containing a Te atom as one of the vertices are very rare. Therefore, our efforts to incorporate main group elements, in particular heavier chalcogen elements, into transition metal cubane and boride clusters have recently been focused on the Te atom. Compound **2**, isostructural with $[(\text{Cp}^*\text{Mo})_2\text{B}_5\text{H}_9]$, was found to be a good precursor for the generation of this type of heterometallic cubane-type and boride clusters. We report herein the synthesis and structural characterization of several unusual molybdaheteroborane clusters with a novel cluster core.

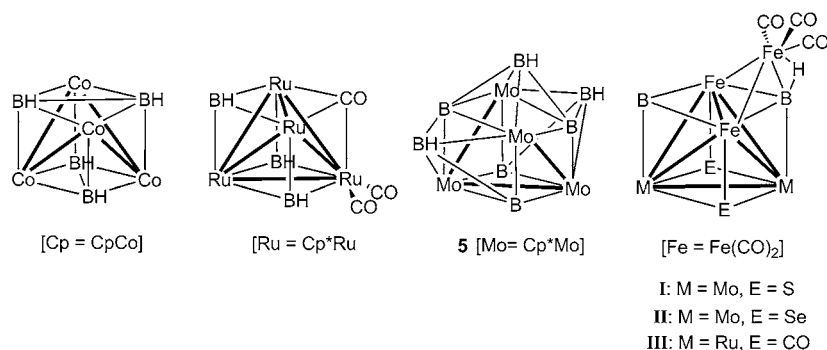
RESULTS AND DISCUSSION

Synthesis of 2–5. As shown in Scheme 1, thermolysis of an in situ generated intermediate, produced from the reaction of $[\text{Cp}^*\text{MoCl}_4]$ ($\text{Cp}^* = \eta^5\text{-C}_5\text{Me}_5$) and $[\text{LiBH}_4\cdot\text{THF}]$ with an

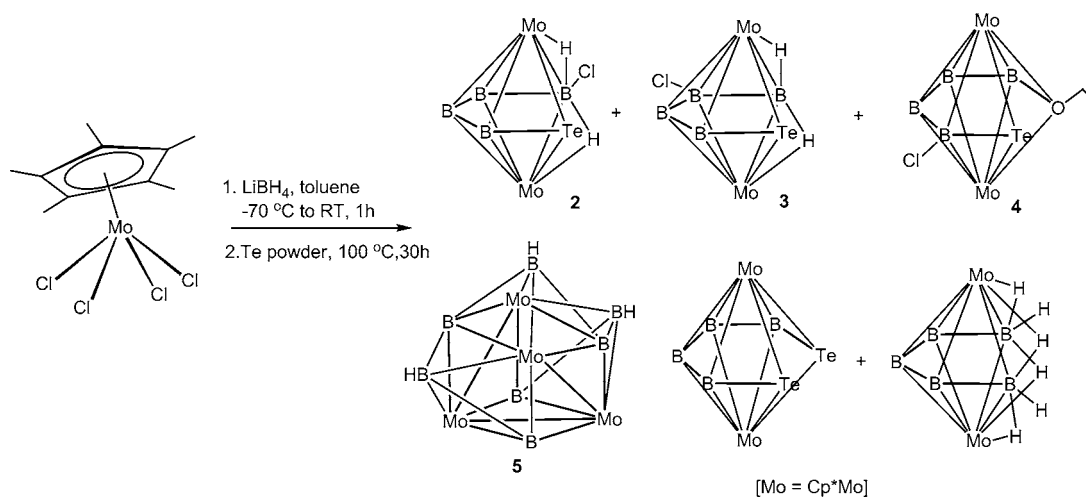
Received: April 27, 2012

Published: July 19, 2012

Chart 1. Metal-Rich Metallaboranes with Cubane-Type Geometry



Scheme 1. Synthesis of Compounds 2–5



excess of Te powder yielded $[(\text{Cp}^*\text{Mo})_2\text{B}_4\text{TeH}_5\text{Cl}]$ (**2** and **3**), $[(\text{Cp}^*\text{Mo})_2\text{B}_4(\mu_3\text{-OEt})\text{TeH}_3\text{Cl}]$ (**4**), and $[(\text{Cp}^*\text{Mo})_4\text{B}_4\text{H}_4(\mu_4\text{-BH})_3]$ (**5**) in moderate to good yields. In parallel with the formation of **2–5** compounds $[(\text{Cp}^*\text{Mo})_2\text{B}_4\text{H}_4\text{Te}_2]$ ¹¹ and $[(\text{Cp}^*\text{Mo})_2\text{B}_5\text{H}_9]$ ¹² have also been isolated in good yields.

The $^{11}\text{B}\{^1\text{H}\}$ NMR spectrum of **2** indicates the presence of four boron resonances at $\delta = 95.5$, 73.2, 40.7, and 26.7 ppm in an intensity ratio of 1:1:1:1. Interestingly, compound **3** also shows four boron resonances at $\delta = 98.8$, 71.8, 51.6, and 24.7 ppm, which are similar to those of $[(\text{Cp}^*\text{Mo})_2\text{B}_4\text{SH}_6]$ and $[(\text{Cp}^*\text{Mo})_2\text{B}_4\text{SeH}_5(\text{Ph})]$.¹³ The peak at $\delta = 40.7$ ppm for **2** and $\delta = 71.8$ ppm for **3** appears as a singlet in the ^{11}B NMR, indicating the absence of terminal hydrogen in boron. Therefore, compounds **2** and **3** could be illustrated as geometrical isomers based on their spectroscopic data. The resonances at $\delta = 26.7$ and 24.7 ppm have been assigned to the unique boron, attached to the tellurium atom. The chemical shift of this boron appeared significantly upfield shifted relative to the S analogue ($\delta = 10.1$ ppm). A similar trend has also been observed in $[(\text{Cp}^*\text{Mo})_2\text{B}_4\text{H}_4\text{E}_2]$ ¹¹ systems (E = S, Se, Te). The upfield chemical shift of these compounds may be due to the electronegativity and size differences between S, Se, and Te. The ^1H NMR spectra of **2** and **3** show the presence of four B–H resonances, one Cp* resonance in the range $\delta = 2.01\text{--}2.11$ ppm and Mo–H–B resonances in the range $\delta = -6.27$ to -6.60 ppm. The ^{13}C NMR spectra also reveal the presence of one type of Cp* resonance. The IR spectra of both **2** and **3** show bands at $2407\text{--}2443\text{ cm}^{-1}$ in a region characteristic of the B–H stretching vibration. Both clusters **2** and **3**, having six

skeleton electron pairs (sep), appear to follow the regular electron-counting rules appropriate for a bicapped trigonal bipyramid.¹⁴

The solid-state structure of one of the isomers (**2**), shown in Figure 1, is fully consistent with the spectroscopic data. All the B–B and Mo–B bond distances are in the normal range. However, the Mo–Mo bond length in **2** is slightly longer (0.03 Å) as compared with the corresponding selenaborane clusters $[(\text{Cp}^*\text{Mo})_2\text{B}_4\text{SeH}_5(\text{Ph})]$. This may be due to the reduced tendency of boron and tellurium atoms to form polarized bonds (compared to boron–oxygen and boron–selenium atoms) that have a localized two-center character, resulting in the observed distances.^{15,16}

$[(\text{Cp}^*\text{Mo})_2\text{B}_4(\mu_3\text{-OEt})\text{TeH}_3\text{Cl}]$, **4.** Compound **4** has been isolated as a brown solid in 4% yield. The ^{11}B NMR spectrum exhibits four boron resonances at $\delta = 87.2$, 77.5, 44.1, and -12.0 ppm with an intensity ratio of 1:1:1:1. The ^1H NMR spectrum shows the presence of three B–H terminal protons and a single Cp* resonance at $\delta = 2.18$ ppm. The $^1\text{H}\{^{11}\text{B}\}$ NMR spectrum displays three singlets in the range $\delta = 7.54\text{--}2.43$ ppm (1:1:1), implying that one of the boron atoms has no terminal hydrogen. In addition to the signal attributable to the $\eta^5\text{-C}_5\text{Me}_5$ protons, the presence of an ethoxy group was also confirmed by the ^1H NMR spectrum. The presence of Cp* and ethoxy moieties was further confirmed by a ^{13}C NMR spectrum. The formation of oxamolybdaborane species is possibly due to the ring-opening insertion of THF into the molybdaborane framework.¹⁷

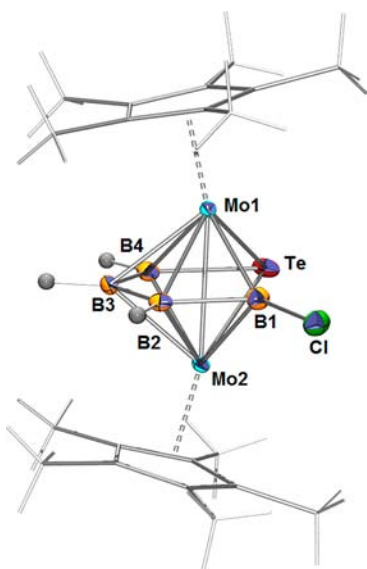


Figure 1. Molecular structure of $[(\text{Cp}^*\text{Mo})_2\text{B}_4\text{H}_5(\mu_3\text{-Te})\text{Cl}]$, **2**. Selected bond lengths (Å) and angles (deg): Mo1–Mo2 2.845(2), B1–B2 1.697(3), B4–Te 2.219(4), Mo2–Te 2.753(2), Mo2–B1 2.155 (6), B1–Cl 1.929(19), Mo2–B4 2.191(9); Mo1–Te–Mo2 81.220(8), B2–B3–B4 114.0(10).

The solid-state structure of **4**, shown in Figure 2, is fully consistent with the spectroscopic data. Although the average

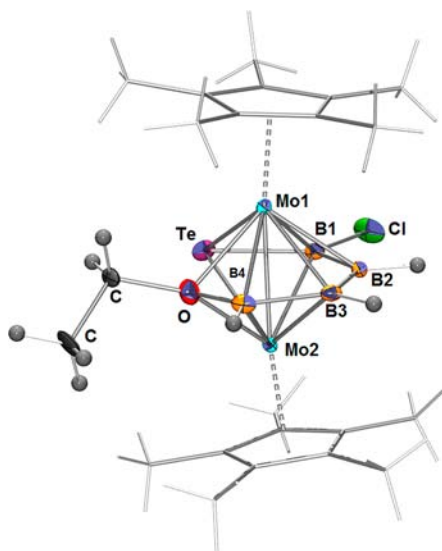


Figure 2. Molecular structure of $[(\text{Cp}^*\text{Mo})_2\text{B}_4(\mu_3\text{-OEt})\text{TeH}_3\text{Cl}]$, **4**. Selected bond lengths (Å) and angles (deg): Mo1–Mo2 2.660(7), Mo1–B2 2.195(7), B1–B2 1.654(10), B4–Te 2.169(8), Mo2–Te 2.759(6), Mo2–B1 2.330(6), B4–O 1.438 (9), Mo2–O 2.140(5); Mo1–Te–Mo2 81.220(8), Mo1–Te–Mo2 76.85(14).

Mo–B (2.281(3) Å) and Mo–Mo bond length (2.6603(7) Å) are comparable to those observed in oxamolybdaborane clusters,¹⁸ they are significantly shorter in comparison with other molybdaborane clusters.^{19,20} This might be due to the presence of an oxygen atom that withdraws electron density from the cluster. The boron–tellurium bond length in **4** was found to be 2.169(8) Å, which is significantly shorter compared to the boron–tellurium bond distance in **2** (2.219(4) Å). Further, the boron–oxygen bond length B4–O1 (1.438(9) Å)

is comparable with other oxamolybdaborane clusters,²¹ but is shorter compared to those observed in other oxametallaborane clusters, for example, 1.523 Å in $[\text{9,9}-(\text{PMe}_2\text{Ph})_2\text{-arachno-9,6-PtOB}_8\text{H}_{10}]$,²² 1.510 Å in $[\text{7}-(\eta^5\text{-C}_5\text{Me}_5)\text{-nido-7,12-RhOB}_{10}\text{H}_9\text{-8-Cl-11}-(\text{PMe}_2\text{Ph})]$,²³ and 1.481 Å in $[\text{2}-(\eta^6\text{-C}_6(\text{CH}_3)_3\text{H}_3)]\text{Fe-O-6-B}_8\text{H}_{10}]$.²⁴ Cluster **4** is unprecedented and a remarkable example of an oxametallaborane containing a heavier group 16 element (Te) as a cluster constituent.

$[(\text{Cp}^*\text{Mo})_4\text{B}_4\text{H}_4(\mu_4\text{-BH})_3]$, **5**. Compound **5** has been isolated in 5% yield as a green solid. The spectroscopic and structural characterization of cluster **5** has been reported in our preliminary communication.²⁵ As shown in Figure 3, the

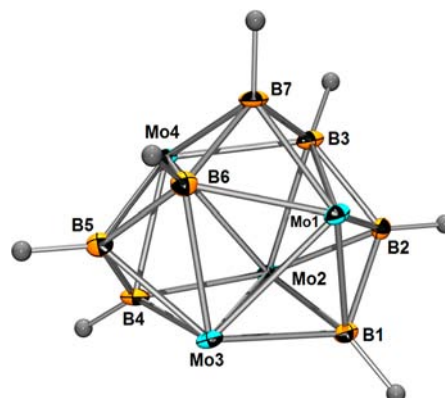
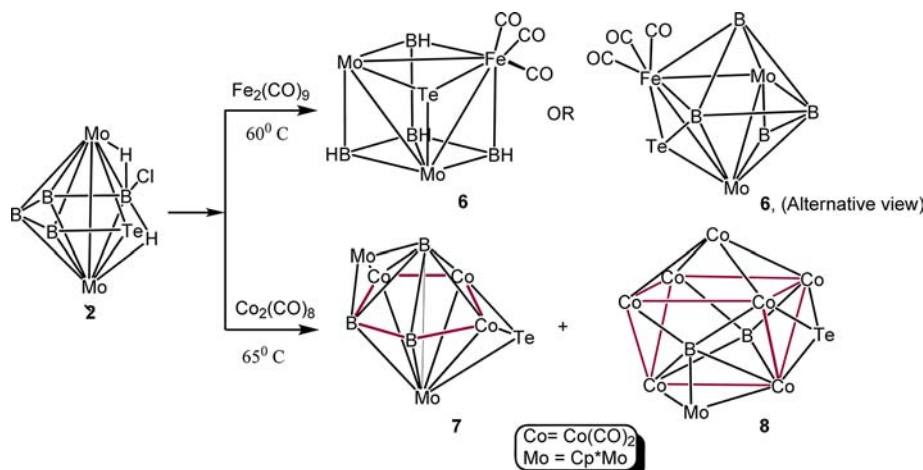


Figure 3. Molecular structure of $[(\text{Cp}^*\text{Mo})_4\text{B}_4\text{H}_4(\mu_4\text{-BH})_3]$, **5**. Cp* are omitted for clarity. Selected bond lengths (Å) and angles (deg): Mo(1)–Mo(3) 2.659 (10), Mo(2)–Mo(4) 2.651 (9), Mo(2)–Mo(3) 2.847(10), Mo(1)–B(1) 2.220(9), Mo(1)–B(2) 2.136(11), Mo(1)–B(3) 2.309(10), Mo(2)–B(2) 2.158(9), Mo(3)–B(6)–Mo(1) 69.71(11).

geometry of **5** can be viewed as cubane, made of four Mo and four B atoms, and out of the six square faces of the cube three of them are capped by BH units to build a $[\text{Mo}_4\text{B}_7]$ core. Alternatively, the observed geometry of **5** can be viewed as a tetracapped tetrahedron in which four molybdenum atoms define a pseudotetrahedron. Compound **5** has five skeleton electron pairs, two electrons fewer for the structure based on a tetrahedron. An alternative electron-counting method is also possible for this cluster. The 11-vertex polyhedron is a deltahedron with six degree 4 vertices for the four molybdenum atoms. The elemental polyhedral topology demands that among the remaining seven vertices two must be of degree 5 and the remaining five must be of degree 4. This is indeed observed in cluster **5**. Alternatively, this structure can be interpreted as a cluster having 24 skeletal electrons required by Wade–Mingos rules for an 11-vertex deltahedron. In counting the skeletal electrons, the three external Mo–Mo bonds indirectly contribute six skeletal electrons by using what would otherwise be lone pair electrons to make the three bonds. Thus, the skeletal electron count for **5** is as follows: 7 BH vertices = 14 skeletal electrons; 4 Cp*Mo vertices using four internal orbitals = 4 skeletal electrons; 3 external Mo–Mo bonds = 6 skeletal electrons; total skeletal electrons = $24 = 2n + 2$ for $n = 11$.

Utilization of $[(\text{Cp}^*\text{Mo})_2\text{B}_4\text{H}_5(\mu_3\text{-Te})\text{Cl}]$, **2, As a Precursor to a Cubane Cluster.** Transition metal carbonyl compounds have received significant attention in polyhedron boranes,²⁶ carboranes,²⁷ metallacarboranes,²⁸ and metallaborane chemistry²⁹ in connection with their potential as versatile

Scheme 2. Synthesis of Heterometallic Cubane **6** and Boride Clusters **7** and **8**^a

^aThe interstitial boron atoms in **8** are not shown for clarity.

reagents in cluster growth reactions. Therefore, upon the availability of **2**, the chemistry was elaborated by means of a cluster expansion reaction with $[\text{Co}_2(\text{CO})_8]$ and $[\text{Fe}_2(\text{CO})_9]$. As shown in Scheme 2, reaction of **2** with $[\text{Fe}_2(\text{CO})_9]$ led to the isolation of a heterometallic cubane-type cluster (**6**) containing Te as one of the vertices.

The solid-state structure of **6**, shown in Figure 4, shows that the cubane core, $\{\text{Mo}_2\text{B}_4\text{FeTe}\}$, is highly distorted. As shown in

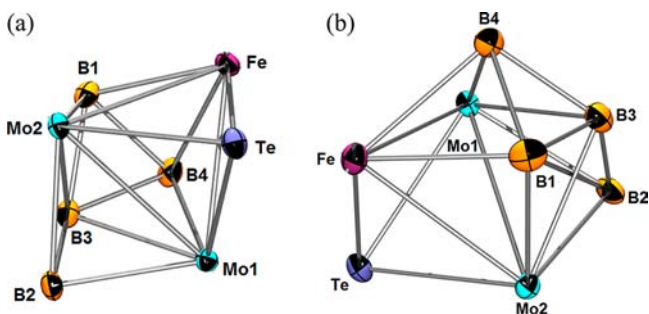


Figure 4. Molecular structure of $[(\text{Cp}^*\text{Mo})_2(\text{BH})_4(\mu_3\text{-Te})\{\text{Fe}(\text{CO})_3\}]$, **6**. Cp^* are not shown for clarity. (a) Cubane view; (b) bicapped octahedron view. Selected bond lengths (Å) and angles (deg): Mo(1)–Mo(2) 2.9518(11), Mo(2)–Te(1) 2.6641(10), Fe(1)–Mo(1) 2.7985(16), Fe(1)–Te(1) 2.6270(15), Mo(1)–B(3) 2.323(11), Fe(1)–B(1) 2.226(13), B(1)–B(2) 1.749(16), B(1)–B(3) 1.741(16); Fe(1)–Te(1)–Mo(2) 64.25(4).

Table 1, the average Mo–Mo bond distance (2.951(9) Å) in cluster **6** is significantly longer than the Mo–Mo bond distances in **5** (2.714 Å) as well as in other single- and double-cubane clusters.³⁰ Alternatively, the observed geometry of **6** can be viewed as a bicapped octahedral structure in which Mo1, Mo2, B1, B3, B4, and Fe, occupying the vertices of the core octahedron, and the two triangular faces Mo1–Mo2–Fe and Mo1–Mo2–B3 are capped by Te and B2, respectively. All the Mo–B and B–B distances are in the normal range for other molybdaborane clusters.^{19,20} The Mo–Fe distances (2.798(16) and 2.813(16) Å) are consistent with the existence of a single bond. The localization of Mo–Mo bonds renders the top four-membered ring (Mo2B1FeTe) and the bottom ring (Mo1B2B3B4) twisted with respect to each other by ca. 1.21°. In this way the B2–Mo2–Te bond angle of the cube is

Table 1. Selected Structural and Spectroscopic Data of **5** and **6** and Other Related Compounds

compound	sep ^a	$d[\text{M}-\text{M}]$ [Å]	$E_{1/2}$	λ_{max}	ref
$[(\text{Cp})_4\text{Ni}_4\text{B}_4\text{H}_4]$	10	2.35 ^b	-	543, 423, 335, 284	9
$[(\text{Cp})_4\text{Co}_4\text{B}_4\text{H}_4]$	8	2.47 ^b	-	548, 365, 302, 257	9
II	6	2.92 ^b	-	-	5
III	6	2.72 ^b	-	-	5
$[(\text{Cp}^*\text{Ru})_3(\mu_3\text{-CO})\text{Co}(\text{CO})_2\text{B}_3\text{H}_3]$	6	2.93 ^c	-	-	10
5	5	2.71 ^b	0.42, 0.63	440, 367, 315, 239	this work
6	7	2.95 ^b	0.16, 0.49	490, 403, 312, 235	this work

^asep = skeletal electron pair. ^bM = Mo. ^cM = Ru.

distorted (92.2(3) Å). Note that the top and bottom four-membered rings of Mo_2B_2 are not planar (dihedral angle 7.74°).

Consistent with the X-ray results, the ¹¹B NMR spectrum of **6** rationalizes the presence of four boron atoms in the ratio 2:1:1 at $\delta = 85.6$, 45.6, and -4.09 ppm, respectively. The ¹¹B{¹H} NMR spectrum of **6** features one downfield resonance at $\delta = 85.6$ ppm, accounting for two four-coordinated boron atoms (B1 and B4). The chemical shifts at $\delta = 45.6$ and -4.09 ppm have been assigned to the five- and three-coordinated boron atoms (B3 and B2), respectively. The ¹H{¹¹B} NMR spectrum reveals three types of B–H protons in the ratio 2:1:1. The ¹H NMR spectral data of **6** suggest a plane of symmetry for a static molecule as well as the presence of a single Cp* resonance at 1.93 ppm. The ¹³C NMR spectrum contains signals attributable to the one type of Cp* ligand and one Fe(CO)₃ fragment. The IR spectrum of **6** shows a band at 2471 cm⁻¹ in a region characteristic for the B–H stretching frequency and three strong bands at 2020, 1971, and 1943 cm⁻¹, which are assigned to the CO stretching modes of the Fe(CO)₃ unit.

The electronic spectrum of compound **6** in the visible region (measured in CH₂Cl₂ solution) shows that there is a single absorption band at 235 nm ($\epsilon = 2700$), with indications of several weaker bands at lower energy. The pattern of this

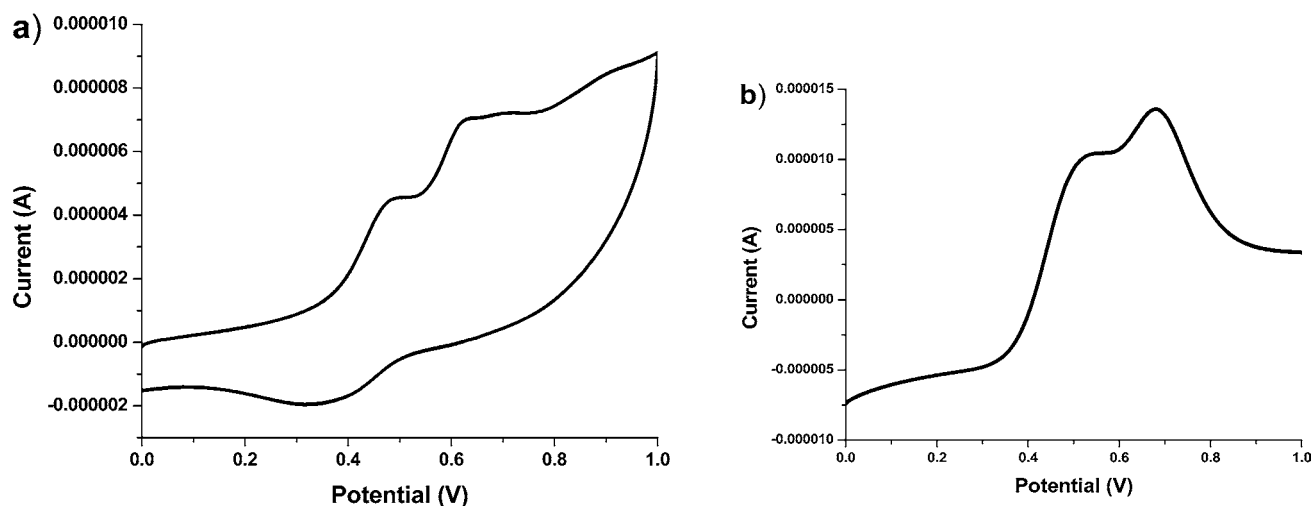


Figure 5. Cyclic voltammetry of compound 6 in CH_2Cl_2 .

spectrum is very similar to those of $[(\text{CpNi})_4\text{B}_4\text{H}_4]$ and 5. As shown in Table 1 (vide infra), the higher intensity band at 235 nm has been blue-shifted by 41 nm on going from $[(\text{CpNi})_4\text{B}_4\text{H}_4]$ to compound 6.³¹ Further, in order to evaluate the redox properties, cyclic voltammetry experiments of cluster 6 were carried out in CH_2Cl_2 using glassy carbon as a working electrode, Pt wire as counter electrode, Ag/Ag^+ as reference electrode, tetrabutylammonium perchlorate as supporting electrolyte, and Fc/Fc^+ as internal standard. The cyclic voltammogram, shown in Figure 5, exhibits one reversible redox potential at $E_{1/2} = 0.42$ V and one quasi-reversible peak at $E_{1/2} = 0.63$ V, which indicate the delocalization nature of metal electrons in the species. Further, differential pulse voltammetry analysis was carried out to obtain the better resolution of redox peaks, and it shows a similar result to that obtained from the CV analysis. For a scan from 0 to 1 V at 50 mV s^{-1} , these redox potentials were probably caused by the dimolybdenum-based reduction processes $[\text{Mo}(\text{II})\text{Mo}(\text{I})/\text{Mo}(\text{I})\text{Mo}(\text{0})]$. On the other hand, compound 5 underwent one quasi-reversible redox along with one reversible redox process at 0.16 V (for S^0/S^+) and 0.49 V ($\text{S}^+/ \text{S}^{2+}$), respectively.

Utilization of $[(\text{Cp}^*\text{Mo})_2\text{B}_3\text{H}_5(\mu_3\text{-Te})\text{Cl}]$, 2, As a Precursor to Boride Clusters. The study of transition metal interstitial borides has produced a richly developed area of cluster chemistry.³² Metallaboranes are predominantly exemplified by boron-rich clusters rather than metal-rich clusters.^{33–39} The characteristic feature that separates the boride clusters⁴⁰ from the metallaboranes is the greater number of boron-to-metal bonding contacts at the expense of boron–hydrogen bonds. Although a number of transition metal clusters containing an encapsulated main group element have been synthesized, only few structurally characterized clusters containing an internal boron atom are known.^{34–39}

The cluster expansion reactions of main group and transition metal polyhedral metallaboranes using a metal carbonyl fragment are well documented.^{41,42} However, examples proceeding in high yield with clean and well-defined stoichiometry are limited. As shown in Scheme 2 (vide infra), compound 2 undergoes a cluster buildup reaction with $[\text{Fe}_2(\text{CO})_9]$ to generate single cubane cluster 6 and on mild thermolysis with an excess of $[\text{Co}_2(\text{CO})_8]$ yielded two heterometallic boride clusters, 7 and 8. Thermolysis of 2 with $[\text{Mn}_2(\text{CO})_{10}]$ and $[\text{Re}_2(\text{CO})_{10}]$ at elevated temperature leads

to the substantial decomposition of compound 2. Clusters 7 and 8 are air-stable brown solids, and they were isolated by thin-layer chromatography (TLC) in 8% and 35% yield, respectively.

$[(\text{Cp}^*\text{MoCO})_2\text{B}_3\text{H}_2(\mu_3\text{-Te})(\mu\text{-CO})\{\text{Co}_3(\text{CO})_6\}]$, 7. The molecular structure of 7, shown in Figure 6, reveals that the cage

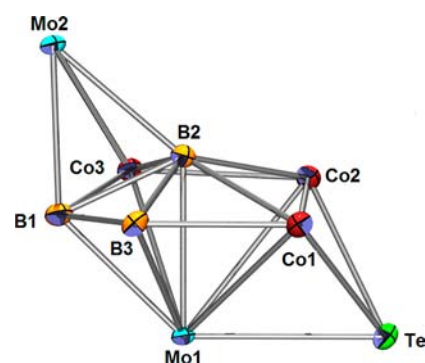


Figure 6. Molecular structure of $[(\text{Cp}^*\text{MoCO})_2\text{B}_3\text{H}_2(\mu_3\text{-Te})(\mu\text{-CO})\{\text{Co}_3(\text{CO})_6\}]$, 7. Cp^* and CO are omitted for clarity. Selected bond lengths (Å) and angles (deg): $\text{Co1}-\text{Co2}$ 2.543(9), $\text{Mo1}-\text{Co3}$ 2.731(7), $\text{Co3}-\text{B1}$ 2.055(5), $\text{Mo2}-\text{B1}$ 2.274(5), $\text{Mo1}-\text{B2}$ 2.315(5); $\text{Co3}-\text{B1}-\text{B3}$ 118.2(3).

geometry is based on a pentagonal bipyramid with a semi-interstitial boron atom. The three cobalt atoms (Co1 , Co2 , and Co3) and two boron atoms (B1 and B3) constitute the pentagonal plane, while the one molybdenum atom (Mo2) and B2 occupy the apical positions of the pentagon. In addition, the triangular faces, $\text{Mo1}-\text{Co1}-\text{Co2}$ and $\text{B1}-\text{B2}-\text{Co3}$, are capped by a Te and Mo1 atom, respectively. Clusters containing bicapped pentagonal bipyramidal geometry are very rare, and only a few examples are known, for example, $[\text{B}_5\text{H}_6\text{Cp}^*\text{Ni}]^{2-}$,⁴³ $[\text{B}_5\text{H}_7(\text{Cp}^*\text{Co})_2]$,⁴⁴ *closo*- $[\text{B}_5\text{H}_4\text{PPh}_3\{\text{Fe}(\text{CO})_3\{\text{Ir}(\text{CO})_2\text{PPh}_3\}]$,⁴⁵ and $[\text{Cp}^*\text{Ir}(\text{B}_3\text{H}_3\text{-C}_2\text{Me}_2)\{\text{Mo}(\text{CO})_3\}(\mu\text{-CO})]$.⁴⁶ Cluster 7 is the first example of this kind of geometry, having Te and a Cp^*Mo fragment occupying the capping positions and boron occupying the semi-interstitial position. The apical $\text{Mo}-\text{B2}$ separation in 7 (2.428(5) Å) is longer than a common $\text{Mo}-\text{B}$ bond (2.21 Å)¹⁴ but comparable with a $\text{Mo}-\text{B}_{\text{equatorial}}$ distance. The $\text{Mo2}_{\text{capping}}-\text{Co3}$ distance is considerably longer (2.987(7) Å) than the average $\text{Mo}-\text{Co}$

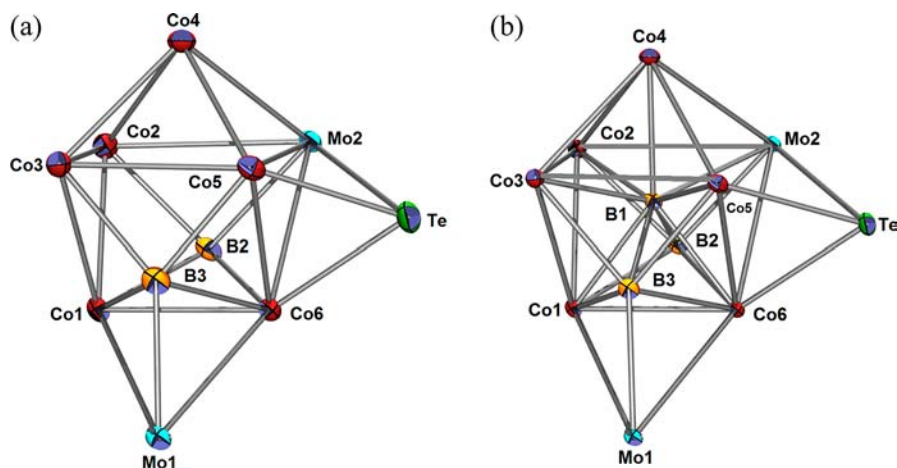


Figure 7. Molecular structure of $[(\text{Cp}^*\text{MoCO})_2\text{B}_3\text{H}_2(\mu_3\text{-Te})(\mu\text{-CO})_4\{\text{Co}_6(\text{CO})_8\}]$, **8**. Cp^* and CO are omitted for clarity. (a) Without interstitial boron atom and (b) with encapsulated boron atom. Selected bond lengths (Å) and angles (deg): Co1-Co2 2.647 (7), Co3-Co5 2.791(6), Mo2-B2 2.280(4), Co5-Co6 2.562(7), Co6-B2 2.109(4), Mo1-Co6 2.731(5), Co5-Te 2.453(5), B1-B2 1.750(5), B1-Co1 2.140(4); Co6-Mo1-Co1 55.604(13).

distance (2.809 Å). The Co1-Co2 distance in the pentagon is 2.543(9) Å, while the internal angles within this pentagon are in the range 97.48(10)–121.74(3)° (107.66° av), comparable with the expected value (108°) for a planar structure.⁴⁷ Indeed, the equatorial Co1-Co2-Co3-B1-B3 ring in **7** is in the plane.

Consistent with the X-ray results, the ^{11}B NMR spectrum of **7** rationalizes the presence of three boron resonances in the ratio 1:1:1. The ^{11}B NMR chemical shift at $\delta = 110$ ppm is tentatively assigned to the unique boron situated at the apical position of the pentagon in a semi-interstitial manner. The ^1H and ^{13}C NMR spectra of **7**, measured at room temperature, are consistent with its unsymmetrical structure. In particular, ^1H NMR spectral data reveal the presence of two kinds of Cp^* signals, and the ^{13}C NMR spectrum confirms the presence of CO . The IR spectrum in the carbonyl region shows both terminal and bridging carbonyl frequencies at 2024, 1996, and 1786 cm^{-1} , which have been assigned to $\text{Co}(\text{CO})_2$ and $\text{Mo}(\text{CO})_2$ fragments, and bands at 2498 and 2368 cm^{-1} are due to the terminal B-H stretches.

$[(\text{Cp}^*\text{MoCO})_2\text{B}_3\text{H}_2(\mu_3\text{-Te})(\mu\text{-CO})_4\{\text{Co}_6(\text{CO})_8\}]$, **8**. Compound **8** was isolated in 35% yield as a brown solid. Single crystals suitable for X-ray diffraction analysis of **8** were obtained from a mixture of hexane and CH_2Cl_2 solution at -10 °C. The crystal structure showed CH_2Cl_2 of solvation. The identity of the heterometallic boride cluster **8** was not easily determined purely on the basis of spectroscopic data, but resolved properly with the support of crystal structure determination. The molecular structure of the boride cluster is shown in Figure 7. The central core of **8** can be regarded as a tetracapped trigonal prism. As shown in Figure 7b, a group of five cobalt and one molybdenum atom forms an idealized trigonal prism with an encapsulated boron atom (B1). Three rectangular faces of the trigonal prism are in turn capped by two boron atoms (B2, B3) and one cobalt atom (Co4), and one of the triangular faces (Mo2-Co5-Co6) is capped by one Te atom. The resulting trigonal face (Co1-B3-Co6) is further capped by one Mo atom; thus molecule **8** can be considered a pentacapped trigonal prism containing 118 cluster valence electrons. Like the M4 butterfly, the M5 square-pyramid, and the M6 octahedron, the trigonal prism framework is not unusual in boride chemistry and was found previously in

$[\text{N}(\text{PPh}_3)_2][\text{Ru}_6\text{H}_2(\text{CO})_{18}\text{B}]^{48}$ and $[\text{AsPh}_4]_2[\text{HFe}_7(\text{CO})_{20}\text{B}]$.⁴⁹ However, the boron-centered trigonal prismatic structure of **8** containing Te and the Cp^*Mo fragment as a capping unit appears to be the first cluster of its type, not only with respect to the environment of the boron atom but also with respect to the metal framework. The boron atom (B1) lies at the center of a trigonal prismatic cage, bonded to six Co atoms, two boron atoms (B2 and B3), and one Mo atom (Mo2). The average Co-Co bond distance (2.592 Å) in the trigonal prismatic core is considerably longer than the sum of the van der Waals radii for metallic cobalt (2.5 Å). The Mo2-Co distances are in the range 2.847(5)–3.010(5) Å, which are significantly longer than the average $\text{Mo}_{\text{capping}}\text{-Co}$ distance (2.771(5) Å).

The X-ray structure of **8** rationalizes the presence of two resonances in the ^{11}B NMR spectrum at $\delta = 166.6$ and 102.1 ppm (1:2). The ^1H NMR spectrum shows one broad signal in the lower field for the terminal BH proton and two sets of distinct chemical shifts for two Cp^* ligands. The ^{13}C NMR spectrum also confirms the presence of two Cp^* ligands and CO groups. The position of the boron chemical shift for B1 ($\delta = 166.6$ ppm) demands some comments. Interstitial boron atoms are usually characterized by their downfield chemical shifts and a sharp signal. Although B1, the interstitial boron atom in **8**, is directly bonded to seven metals, the ^{11}B NMR chemical shifts appear comparatively upfield.⁴⁹ This may be due to the change in connectivity associated with the interstitial boron (B1), which is also directly linked to two boron atoms. Resonances of relative intensity two at $\delta = 102.1$ ppm can be assigned to the five- and six-connected boron atoms (B2 and B3). The IR spectrum shows the presence of characteristic stretching frequencies for CO groups attached to Mo and Co atoms.

CONCLUSION

We report herein the synthesis and structural characterization of two novel dimolybdatelluraborane clusters (**2** and **3**) and systematic study of the reactivity of one of the isomers (**2**) with metal carbonyl compounds. Dimolybdoxatelluraborane **4** has its tellurium and oxygen atom in the open-face position of cluster connectivity three, and this is unprecedented. Compound **5** is a novel example of a homometallic cuboidal

Table 2. Crystallographic Data and Structure Refinement Information for Compounds 2 and 4–8

	2	4	5	6	7	8
empirical formula	C ₂₀ H ₃₅ B ₄ TeClMo ₂	C ₂₂ H ₃₈ B ₄ ClOMo ₂ Te	C ₄₀ H ₆₇ B ₇ Mo ₄	C ₂₅ H ₃₄ B ₄ FeTeO ₅ Mo ₂	C ₂₉ H ₃₂ B ₃ TeO ₉ Mo ₂ Co ₃	C ₃₄ H ₃₂ B ₃ TeO ₁₄ Mo ₂ Co ₆
fw	671.63	714.96	1007.37	831.305	1050.28	1368.024
cryst syst	orthorhombic	orthorhombic	triclinic	monoclinic	triclinic	monoclinic
space group	<i>Pbca</i>	<i>Pbca</i>	<i>P</i> $\bar{1}$	<i>P2(1)/n</i>	<i>P</i> $\bar{1}$	<i>P2(1)/n</i>
<i>a</i> (Å)	14.900(3)	15.2196(4)	11.2490(7)	8.5599(5)	10.3465(7)	11.0344(4)
<i>b</i> (Å)	21.774(4)	16.0129(3)	11.9722(8)	15.6973(10)	11.6799(7)	17.3088(7)
<i>c</i> (Å)	16.047(3)	22.6286(5)	18.7227(12)	20.8469(11)	16.5804(10)	23.3171(9)
α (deg)	90.00	90.00	77.172(3)	90.00	74.313(3)	90.00
β (deg)	90.00	90.00	86.647(3)	90.292	76.110(3)	91.414(2)
γ (deg)	90.00	90.00	87.738(3)	90.00	63.926(3)	90.00
<i>V</i> (Å ³)	5206.2(18)	5514.8(2)	2455.1(3)	2801.1(3)	1715.62(19)	4452.0(3)
<i>Z</i>	8	8	2	4	2	4
<i>D</i> _{calc} (g/cm ³)	1.714	1.711	1.363	1.833	2.035	2.168
<i>F</i> (000)	2568	2808	1020	1496	1016	2804
μ (mm ⁻¹)	1.619	2.056	1.022	2.436	3.014	3.547
cryst size (mm)	0.20 × 0.15 × 0.10	0.35 × 0.32 × 0.10	0.25 × 0.22 × 0.10	0.15 × 0.10 × 0.08	0.20 × 0.18 × 0.10	0.42 × 0.35 × 0.20
θ range (deg)	2.6–24.50	2.8–26.5	2.05–28.05	2.35–28.30	2.40–30.12	2.51–34.73
no. of unique reflns collected	4580	4831	8424	6347	9662	13 016
goodness-of-fit on <i>F</i> ²	1.189	1.119	1.111	1.108	0.977	1.080
final <i>R</i> indices [<i>I</i> > 2 σ (<i>I</i>)]	<i>R</i> ₁ = 0.0448	<i>R</i> ₁ = 0.0405	<i>R</i> ₁ = 0.0624	<i>R</i> ₁ = 0.0688	<i>R</i> ₁ = 0.0456	<i>R</i> ₁ = 0.0366
	<i>wR</i> ₂ = 0.1054	<i>wR</i> ₂ = 0.0983	<i>wR</i> ₂ = 0.1791	<i>wR</i> ₂ = 0.2021	<i>wR</i> ₂ = 0.1047	<i>wR</i> ₂ = 0.1295
<i>R</i> indices (all data)	<i>R</i> ₁ = 0.0583	<i>R</i> ₁ = 0.0636	<i>R</i> ₁ = 0.0859	<i>R</i> ₁ = 0.0837	<i>R</i> ₁ = 0.0729	<i>R</i> ₁ = 0.0453
	<i>wR</i> ₂ = 0.1100	<i>wR</i> ₂ = 0.1162	<i>wR</i> ₂ = 0.2077	<i>wR</i> ₂ = 0.2110	<i>wR</i> ₂ = 0.1179	<i>wR</i> ₂ = 0.1390

metallaborane cluster containing boron as a main group element, whereas compound **6** is a heterometallic cuboidal metallaborane cluster containing a Te atom as one of the vertices. The clusters **7** and **8** are notable examples of heterometallic boride clusters having one semi-interstitial boron and one completely encapsulated boron atom, respectively.

EXPERIMENTAL SECTION

General Procedures and Instrumentation. All manipulations were conducted either under an atmosphere of dry argon inside a glovebox or employing standard Schlenk techniques. Solvents were distilled prior to use under argon. [Mo(CO)₆], [PCl₅], [Fe₂(CO)₉], [Mn₂(CO)₁₀], [Co₂(CO)₈], and LiBH₄ in THF (Aldrich) were used as received. The [Cp*MoCl₄] complex was prepared as described in the literature.⁵⁰ The external reference for the ¹¹B NMR, [Bu₄N-(B₃H₈)], was synthesized with the literature method.⁵¹ Thin-layer chromatography was carried on 250 mm diameter aluminum-supported silica gel TLC plates (Merck). The NMR spectra were recorded in a 400 MHz Bruker FT-NMR spectrometer. Residual solvent protons were used as reference (δ , ppm, benzene, 7.16), while a sealed tube containing [Bu₄N(B₃H₈)] in benzene-*d*₆ (δ _B, ppm, -30.07) was used as an external reference for the ¹¹B NMR. Infrared spectra were recorded on a Nicolet iS10 FT spectrometer. The absorption spectra were recorded with a JASCO V-650 UV-vis spectrophotometer at 298 K. The CV measurements were performed in a CH potentiostat model 668. Microanalyses for C, H, and N were performed on a Perkin Elmer Instruments series II model 2400.

Synthesis of 2–5. In a flame-dried Schlenk tube, [Cp*MoCl₄] (0.5 g, 1.34 mmol) was suspended in toluene (20 mL) and cooled to -78 °C. LiBH₄·THF (4.02 mL, 8.05 mmol) was added slowly, and the reaction mixture was warmed slowly over 20 min to room temperature and left stirring for an additional hour. The solvent was removed under

reduced pressure, and the residue was extracted into hexane. The yellowish-green hexane extract was thermolyzed at 100 °C with an excess of Te powder (0.683 g, 5.36 mmol) in toluene for 30 h. The solvent was removed in vacuo, and the residue was extracted into hexane. After removal of solvent from the filtrate, the residue was subjected to chromatographic workup using silica gel TLC plates. Elution with hexane/CH₂Cl₂ (95:05 v/v) yielded green **2** and **3** (**2**, 0.112 g, 25%; **3**, 0.030 g, 6%), brown **4** (0.023 g, 4%), and green **5** (0.038 g, 5%). Note that, along with the formation of **2–5**, known [(Cp*Mo)₂B₄Te₂H₄] (0.03 g, 6%) and [(Cp*Mo)₂B₅H₉] (0.08 g, 24%) have also been isolated.

Compound 2. ¹¹B NMR (128 MHz, [D₆]benzene, 22 °C): δ 95.5 (s, br, 1B), 73.2 (s, br, 1B), 40.7 (s, br, 1B), 26.7 (s, br, 1B). ¹H NMR (400 MHz, [D₆]benzene, 22 °C): δ 8.33 (partially collapsed quartet (pcq), 1BH_t), 4.80 (pcq, 1BH_t), 3.43 (pcq, 1BH_t), 2.01 (s, 30H, C₅Me₅), -6.60 (s, 2H, Mo–H–B). ¹³C NMR (100 MHz, [D₆]benzene, 22 °C): δ 107.34 (C₅(CH₃)₅), 12.76 (C₅(CH₃)₅). IR (hexane, cm⁻¹): 2443w, 2407w cm⁻¹ (B–H). Anal. Calcd (%) for C₂₀H₃₅B₄TeClMo₂: C 35.66, H 5.24. Found: C 36.23, H 4.99.

Compound 3. ¹¹B NMR (128 MHz, [D₆]benzene, 22 °C): δ 98.8 (s, br, 1B), 71.8 (s, br, 1B), 51.6 (s, br, 1B), 24.7 (s, br, 1B). ¹H NMR (400 MHz, [D₆]benzene, 22 °C): δ 8.25 (partially collapsed quartet (pcq), 1BH_t), 4.81 (pcq, 1BH_t), 3.43 (pcq, 1BH_t), 2.11 (s, 30H, C₅Me₅), -6.27 (s, 2H, Mo–H–B). ¹³C NMR (100 MHz, [D₆]benzene, 22 °C): δ 108.69 (C₅(CH₃)₅), 13.63 (C₅(CH₃)₅). IR (hexane, cm⁻¹): 2431w, 2417w cm⁻¹ (B–H). Anal. calcd (%) for C₂₀H₃₅B₄TeClMo₂: C 35.66, H 5.24. Found: C 36.13, H 5.06.

Compound 4. ¹¹B NMR (128 MHz, [D₆]benzene, 22 °C): δ 87.2 (s, br, 1B), 77.5 (s, br, 1B), 44.1 (s, br, 2B), -12.0 (s, br, 1B). ¹H NMR (400 MHz, [D₆]benzene, 22 °C): δ 7.54 (partially collapsed quartet (pcq), 1BH_t), 2.80 (pcq, 1BH_t), 2.43 (pcq, 1BH_t), 2.18 (s, 30H, C₅Me₅), -6.70 (s, 4H, Mo–H–B). ¹³C NMR (100 MHz, [D₆]benzene, 22 °C): δ 105.7 (C₅(CH₃)₅), 12.7 (C₅(CH₃)₅). IR (hexane, cm⁻¹): 2413w, 2397w cm⁻¹ (B–H).

Compound 5. ^{11}B NMR (128 MHz, $[\text{D}_6]$ benzene, 22 °C): δ 131.5 (s, br, 2B), 94.5 (s, br, 2B), 58.8 (s, br, 3B). ^1H NMR (400 MHz, $[\text{D}_6]$ benzene, 22 °C): δ 9.92 (partially collapsed quartet (pcq), 2BH_i), 8.93 (pcq, 2BH_i), 6.12 (pcq, 3BH_i), 2.14 (s, 15H, C₅Me₃), 1.58 (s, 15H, C₅Me₃). ^{13}C NMR (100 MHz, $[\text{D}_6]$ benzene, 22 °C): δ 105.8 (C₅(CH₃)₅), 103.4 (C₅(CH₃)₅), 14.0 (C₅(CH₃)₅), 12.6 (C₅(CH₃)₅). IR (hexane, cm⁻¹): 2490w, 2471w cm⁻¹ (B–H_i). Anal. Calcd (%) for C₂₀H₃₅B₄TeClMo₂: C 47.64, H 6.65. Found: C 47.13, H 5.94.

Synthesis of 6. A solution of **2** (0.15 g, 0.23 mmol) in hexane (15 mL) was stirred at 70 °C in the presence of 3 equivalents of $[\text{Fe}_2(\text{CO})_9]$ (0.25 g, 0.69 mmol) for 3 h. The solvent was removed in vacuo, and the residue was extracted into hexane and passed through Celite. The filtrate was concentrated and kept at –40 °C to remove Fe₃(CO)₁₂. The mother liquor was concentrated, and the residue was chromatographed on silica gel TLC plates. Elution with a hexane/CH₂Cl₂ (8:2 v/v) mixture yielded yellow **6** (0.028 g, 15%).

Compound 6. ^{11}B NMR (128 MHz, $[\text{D}_6]$ benzene, 22 °C): δ 85.6 (br, 2B), 45.6 (br, 1B), –4.09 (br, 1B). ^1H NMR (400 MHz, $[\text{D}_6]$ benzene, 22 °C): δ 8.28 (br, 1BH_i), 4.34 (br, 1BH_i), 1.93 ppm (s, 30H, Cp*). ^{13}C NMR (100 MHz, $[\text{D}_6]$ benzene, 22 °C): δ 221.6 (CO), 205.1 (CO), 106.2 (C₅(CH₃)₅), 11.6 (C₅(CH₃)₅). IR (hexane, cm⁻¹): 2471 (w, B–H_i), 2020, 1971, 1943 cm⁻¹ (CO). Anal. Calcd (%) for C₂₃H₃₄B₄FeTeO₃Mo₂: C 35.85, H 4.41. Found: C 36.68, H 4.29.

Synthesis of 7 and 8. A yellow solution of compound **2** (0.15 g, 0.23 mmol) in hexane (15 mL) was stirred at 70 °C in the presence of 3 equivalents of $[\text{Co}_2(\text{CO})_8]$ (0.235 g, 0.69 mmol) for 6 h. All volatiles were removed in vacuo, and the residue was extracted into hexane, and passed through Celite. The mother liquor was concentrated, and the residue was chromatographed on silica gel TLC plates. Elution with hexane/CH₂Cl₂ (8:2 v/v) yielded brown **7** (0.018 g, 8%) and **8** (0.107 g, 35%).

Compound 7. ^{11}B NMR (128 MHz, $[\text{D}_6]$ benzene, 22 °C): δ 110.0 (s, 1B), 91.3 (br, 1B), 76.2 (br, 1B) ppm. ^1H NMR (400 MHz, $[\text{D}_6]$ benzene, 22 °C): δ 7.29 (br, 1BH_i), 7.32 (br, 1BH_i), 2.08 (s, 15H, Cp*), 1.98 (s, 15H, Cp*). ^{13}C NMR (100 MHz, $[\text{D}_6]$ benzene, 22 °C): δ 229.3 (CO), 201.1 (CO), 196.6 (CO), 106.5, 107.6 (C₅(CH₃)₅), 12.6, 13.4 (C₅(CH₃)₅). IR (hexane, cm⁻¹): 2498, 2368 cm⁻¹ (w, B–H_i), 2024, 1996, 1786 cm⁻¹ (CO). Anal. Calcd (%) for C₂₉H₃₂B₃TeO₉Mo₂Co₃: C 33.13, H 3.04. Found: C 31.96, H 2.92.

Compound 8. ^{11}B NMR (128 MHz, $[\text{D}_6]$ benzene, 22 °C): δ 166.6 (br, 1B), 102.1 (br, 2B). ^1H NMR (400 MHz, $[\text{D}_6]$ benzene, 22 °C): δ 8.32 (br, 1BH_i), 2.08 (s, 15H, Cp*), 2.18 (s, 15H, Cp*). ^{13}C NMR (100 MHz, $[\text{D}_6]$ benzene, 22 °C): δ 219.3, 205.4, 198.0 (CO), 104.5, 102.7 (C₅(CH₃)₅), 11.2, 9.8 (C₅(CH₃)₅). IR (hexane, cm⁻¹): 2498, 2364 (w, B–H_i), 2013, 1993, 1736 cm⁻¹ (CO). Anal. Calcd (%) for C₃₄H₃₂B₃TeO₁₄Mo₂Co₆: C 29.80, H 2.35. Found: C 30.21, H 2.12.

X-ray Structure Determination. Crystallographic information for the compounds is given in Table 2. The crystal data for **2** and **4–8** were collected and integrated using a Bruker Axs kappa apex2 CCD diffractometer, with graphite-monochromated Mo K α ($\lambda = 0.71073$ Å) radiation at 173 K. The structures were solved by heavy atom methods using SHELXS-97 or SIR92⁵² and refined using SHELXL-97.⁵³

■ ASSOCIATED CONTENT

Ⓢ Supporting Information

Supplementary crystallographic data and X-ray crystallographic files for **2** and **4–8**. This material is available free of charge via the Internet at <http://pubs.acs.org>.

■ AUTHOR INFORMATION

Corresponding Author

*Phone: (+91) 44 2257 4230. Fax: (+91) 44 2257 4202. E-mail: sghosh@iitm.ac.in.

Notes

The authors declare no competing financial interest.

■ ACKNOWLEDGMENTS

Generous support of the Indo-French Centre for the Promotion of Advanced Research (IFCPAR-CEFIPRA), No. 4405-1, New Delhi, is gratefully acknowledged. A.T. thanks the Council of Scientific and Industrial Research (CSIR), India, for a Senior Research Fellowship. We would like to thank Dr. Babu Varghese for X-ray crystallography analysis and Dr. Ramanujam Kothandaraman of Indian Institute of Technology, Madras, for helpful discussions on electrochemistry.

■ REFERENCES

- (1) Whitmire, K. H. *J. Coord. Chem.* **1998**, *17*, 95.
- (2) Fedin, V. P.; Czyzniewska, J.; Prins, R.; Weber, T. *Appl. Catal., A* **2001**, *213*, 123.
- (3) *Transition Metal Sulfides Chemistry and Catalysis*; Weber, T.; Prins, R.; van Santen, R. A., Eds.; Kluwer: Dordrecht, 1998.
- (4) (a) Holm, R. H. *Adv. Inorg. Chem.* **1992**, *38*, 1–71. (b) Shibahara, T. *Adv. Inorg. Chem.* **1991**, *37*, 143.
- (5) Geetharani, K.; Bose, S. K.; Sahoo, S.; Ghosh, S. *Angew. Chem.* **2011**, *123*, 3994.
- (6) Trinh, T.; Teo, B. K.; Ferguson, J. A.; Meyer, T. J.; Dahl, L. F. *J. Am. Chem. Soc.* **1977**, *99*, 408.
- (7) Houser, E. J.; Amarasekera, J.; Rauchfuss, T. B.; Wilson, S. R. *J. Am. Chem. Soc.* **1991**, *113*, 7440.
- (8) Inomata, S.; Tobita, H.; Ogino, H. *J. Am. Chem. Soc.* **1990**, *112*, 6145.
- (9) (a) Bowser, J. R.; Bonny, A.; Pipal, J. R.; Grimes, R. N. *J. Am. Chem. Soc.* **1979**, *101*, 6229. (b) Pipal, J. R.; Grimes, R. N. *Inorg. Chem.* **1979**, *18*, 257.
- (10) Lei, X.; Shang, M.; Fehlner, T. P. *Organometallics* **2000**, *19*, 4429.
- (11) Sahoo, S.; Mobin, S. K.; Ghosh, S. *J. Organomet. Chem.* **2009**, *695*, 945.
- (12) Weller, A. S.; Shang, M.; Fehlner, T. P. *Organometallics* **1999**, *18*, 853.
- (13) Dhayal, R. S.; Ramkumar, V.; Ghosh, S. *Polyhedron* **2011**, *30*, 2062.
- (14) (a) Aldridge, S.; Hashimoto, H.; Kawamura, K.; Shang, M.; Fehlner, T. P. *Inorg. Chem.* **1998**, *37*, 928. (b) Bullick, H. J.; Grebenik, P. D.; Green, M. L. H.; Hughes, A. K.; Leach, J. B.; McGowan, P. C. *J. Chem. Soc., Dalton Trans.* **1995**, *67*. (c) Aldridge, S.; Shang, M.; Fehlner, T. P. *J. Am. Chem. Soc.* **1998**, *120*, 2586.
- (15) Bicerano, J.; Lipscomb, W. N. *Inorg. Chem.* **1980**, *19*, 1825.
- (16) Dolansky, J.; Hermanek, S.; Zahradnik, R. *Collect. Czech. Chem. Commun.* **1981**, *46*, 2479.
- (17) (a) Borodinsky, L.; Grimes, R. N. *Inorg. Chem.* **1982**, *21*, 1921. (b) Hodson, B. E.; McGrath, T. D.; Stone, F. G. A. *Organometallics* **2005**, *24*, 1638.
- (18) (a) Micciche, R. P.; Briguglio, J. J.; Sneddon, L. G. *Inorg. Chem.* **1984**, *23*, 3992. (b) Kim, Y. -H.; Brownless, A.; Cooke, P.; Greatrex, A. R.; Kennedy, J. D.; Thornton-Pett, M. *Inorg. Chem. Commun.* **1998**, *1*, 19. (c) Ditzel, E. J.; Fontaine, X. L. R.; Fowkes, H.; Greenwood, N. N.; Kennedy, J.; MacKinnon, D.; Sisan, P. Z.; Thornton-Pett, M. *J. Chem. Soc., Chem. Commun.* **1990**, 1692.
- (19) Aldridge, S.; Shang, M.; Fehlner, T. P. *J. Am. Chem. Soc.* **1998**, *120*, 2586.
- (20) Bullick, H. J.; Grebenik, P. D.; Green, M. L. H.; Hughes, A. K.; Leach, J. B.; McGowan, P. C. *J. Chem. Soc., Dalton Trans.* **1995**, *67*.
- (21) Sahoo, S.; Dhayal, R. S.; Varghese, B.; Ghosh, S. *Organometallics* **2009**, *28*, 1586.
- (22) Kim, Y. -H.; Brownless, A.; Cooke, P. A.; Greatrex, R.; Kennedy, J. D.; Thornton-Pett, M. *Inorg. Chem. Commun.* **1998**, *1*, 19.
- (23) Fontaine, X. L. R.; Fowkes, H.; Greenwood, N. N.; Kennedy, J. D.; Thornton-Pett, M. *J. Chem. Soc., Dalton Trans.* **1987**, 2417.
- (24) Micciche, R. P.; Briguglio, J. J.; Sneddon, L. G. *Inorg. Chem.* **1984**, *23*, 3992.
- (25) Thakur, A.; Sahoo, S.; Ghosh, S. *Inorg. Chem.* **2011**, *50*, 7940.

- (26) (a) Kennedy, J. D. *Prog. Inorg. Chem.* **1984**, *32*, 519.
(b) Kennedy, J. D. *Prog. Inorg. Chem.* **1986**, *34*, 211.
- (27) (a) Grimes, R. N. *Appl. Organomet. Chem.* **1996**, *10*, 209.
(b) Hosmane, N. S. In *Advances in Boron Chemistry*; Siebert, W., Ed.; Royal Society of Chemistry: Cambridge, U.K., 1997; p 349.
- (28) Grimes, R. N. In *Comprehensive Organometallic Chemistry II*; Wilkinson, G.; Abel, E.; Stone, F. G. A., Eds.; Pergamon: Oxford, England, 1995; Vol. 1, Chapter 9, p 373.
- (29) (a) Grimes, R. N. *Coord. Chem. Rev.* **1995**, *143*, 71. (b) Grimes, R. N. *Coord. Chem. Rev.* **2000**, *200*, 773. (c) Deng, L.; Xie, Z. *Coord. Chem. Rev.* **2007**, *251*, 2452.
- (30) (a) Feliz, M.; Guillamón, E.; Llusar, R.; Vicent, C.; Stiriba, S. E.; Pérez-Prieto, J.; Barberis, M. *Chem.—Eur. J.* **2006**, *12*, 1486. (b) Curtis, M. D.; Riaz, U.; Curnow, O. J.; Kampf, J.; Rheingold, W. A. L.; Haggerty, B. S. *Organometallics* **1995**, *14*, 5337.
- (31) This may be due to the presence of the $\{\eta^5\text{-C}_5(\text{CH}_3)_5\}$ ligand, which generally produces a stronger ligand field than the $\{\eta^5\text{-C}_5\text{H}_5\}$ ligand. The high-energy band at 235 nm may be attributed to a metal to ligand charge transfer transition (MLCT), whereas the lower energy bands at 312 and 403 nm may be assigned to ligand to a metal charge transfer transition (LMCT).
- (32) Housecroft, C. E. *Coord. Chem. Rev.* **1995**, *143*, 297.
- (33) (a) Housecroft, C. E. *Adv. Organomet. Chem.* **1991**, *33*, 1–50.
(b) Housecroft, C. E. *Polyhedron* **1987**, *6*, 1935–1958.
- (34) Braunschweig, H. R.; Dewhurst, D.; Kraft, K.; Radacki, K. *Angew. Chem., Int. Ed.* **2009**, *48*, 5837.
- (35) Hong, F.-E.; Coffy, T. J.; McCarthy, D. A.; Shore, S. G. *Inorg. Chem.* **1989**, *28*, 3284.
- (36) Chung, J. H.; Jordan, G.; Meyers, E. A.; Shore, S. G. *Inorg. Chem.* **2000**, *39*, 568.
- (37) Khattar, R.; Puga, J.; Fehlner, T. P. *J. Am. Chem. Soc.* **1989**, *111*, 1877.
- (38) Bandyopadhyay, A.; Khattar, R.; Puga, J.; Fehlner, T. P.; Rheingold, A. L. *Inorg. Chem.* **1992**, *31*, 465.
- (39) Bühl, M.; Schleyer, P. V. R. *J. Am. Chem. Soc.* **1992**, *114*, 477.
- (40) Wong, K. S.; Scheidt, W. R.; Fehlner, T. P. *J. Am. Chem. Soc.* **1982**, *104*, 1111.
- (41) (a) Housecroft, C. E. *Boranes and Metalloboranes*; Ellis Horwood: Chichester, U.K., 1990. (b) Shriver, D. F.; Kaesz, H. D. In *The Chemistry of Metal Cluster Complexes*; Adams, R. D., Ed.; VCH: New York, 1990.
- (42) Ghosh, S.; Fehlner, T. P.; Noll, B. C. *Chem. Commun.* **2005**, 3080.
- (43) Vinitskii, D. M.; Lagun, V. L.; Solntsev, K. A.; Kuznetsov, N. T.; Marushkin, K. N.; Janousek, J.; Base, K.; Stibr, B. *Russ. J. Inorg. Chem.* **1984**, *29*, 984.
- (44) Venable, T. L.; Grimes, R. N. *Inorg. Chem.* **1982**, *21*, 887.
- (45) Bould, J.; Rath, N. P.; Fang, H.; Barton, L. *Inorg. Chem.* **1996**, *35*, 2062.
- (46) Montigny, F.; De.; Macias, R.; Noll, B. C.; Fehlner, T. P. *Angew. Chem., Int. Ed.* **2006**, *45*, 2119.
- (47) Rivard, E.; Steiner, J.; Fettingner, J. C.; Giuliani, J. R.; Augustine, M. P.; Power, P. P. *Chem. Commun.* **2007**, 4919.
- (48) Housecroft, C. E.; Matthews, D. M.; Rheingold, A. L.; Song, X. *J. Chem. Soc. Chem. Commun.* **1992**, 842.
- (49) Bandyopadhyay, A.; Shang, M.; Jun, C. S.; Fehlner, T. P. *Inorg. Chem.* **1994**, *33*, 3677.
- (50) Green, M. L. H.; Hubert, J. D.; Mountford, P. *J. Chem. Soc., Dalton Trans.* **1990**, 3793.
- (51) Ryschkewitsch, G. E.; Nainan, K. C. *Inorg. Synth.* **1974**, *15*, 113.
- (52) Sheldrick, G. M. *SHELXS-97*; University of Göttingen: Germany, 1997.
- (53) Sheldrick, G. M. *SHELXL-97*; University of Göttingen: Germany, 1997.